

Quantitative Determination of the Critical Points of Mott Metal-Insulator Transition in Strongly Correlated Systems

Yuekun Niu^{1,*}, Yu Ni², Jianli Wang¹, Leiming Chen¹, Ye Xing¹, Yun Song^{2,†} and Shiping Feng^{2,‡}

¹*School of Materials Science and Physics, China University of Mining and Technology, Xuzhou, 221116, China*

²*Department of Physics, Beijing Normal University, Beijing 100875, China*

The Mottness is at the heart of the essential physics in a strongly correlated system as many novel quantum phenomena occur at the metallic phase near the Mott metal-insulator transition. We investigate the Mott metal-insulator transition in a strongly-correlated electron system based on the Hubbard model. The on-site moment evaluated by the dynamical mean-field theory is employed to depict the Mott metal-insulator transition. Conveniently, the on-site moment is a more proper order parameter to quantitatively determine the Mott critical point, in comparison with the corresponding quasiparticle coherent weight. Moreover, this order parameter also gives a consistent description of two distinct forms of the critical points of the Mott metal-insulator transition.

PACS numbers: 71.30.+h, 71.27.+a, 71.50.+t

Introduction. The Mott metal-insulator transition (MIT) [1–3] driven by a competition between the kinetic energy t of the electrons and the on-site Coulomb repulsive interaction U between electrons is a paradigmatic example of the strong electron correlation effect. In particular, it has been shown experimentally that the unconventional superconductivity and many other exotic quantum phenomena occur at the metallic phase near the Mott MIT [3]. This is why the quantitative determination of the critical point of the Mott MIT is crucial to deeply understand the essential physics of the novel quantum phenomena in a strong correlation system.

Although the intense efforts at the experimental and theoretical levels have been put forth in order to understand the physical origin of the Mott MIT together with the associated novel quantum phenomena [3], the quantitative determination of the critical point of the Mott MIT still is a challenging issue. In the early studies, it has been shown in the Gutzwiller approximation that the quasiparticle coherent weight can be identical as the order parameter to determine the critical point of the Mott MIT, where the quasiparticle coherent weight Z_F disappears and the effective mass diverges as $1/Z_F$ when the strength of the Coulomb interaction approaches its value at the critical point of MIT [4, 5]. This is followed a fact that the quasiparticle coherent peak around the Fermi surface comes mainly from the scattering of electrons on the local-spin fluctuations, and then its disappearance at the critical point of MIT can be also tracked by analyzing the energy dependence of the electron self-energy at different Coulomb repulsive interactions [6]. Later on, the systematic analysis [7] based on the dynamical mean-field theory (DMFT) indicates that at low-temperature, the opening of the gap and the vanishing of the quasiparticle coherent peak do not happen at the same critical value of U_c , instead, MIT is found as a function of U/t , with the corresponding metallic and insulating solutions coexisting between U_{c2} and U_{c1} , respectively. Since then, a series of studies focused on the region of the metallic and

insulating solutions coexisting between U_{c2} and U_{c1} has been made [8–14]. However, these studies also indicate that the quasiparticle coherent weight Z_F as an order parameter may not be able to mark off these two distinct forms of the critical points in MIT conveniently, due to the coexistence of a branch of metastable metallic solution that connect the two stable metallic and insulating solutions of Z_F [15, 16]. In this case, a natural question is raised: is there a more proper order parameter to define the existence of two distinct forms of the critical points in the Mott MIT?

In this paper, we study the Mott MIT in a strongly correlated system based on DMFT with the *Lanczos* method as impurity solver, and show that the on-site moment is a more proper order parameter to quantitatively determine the critical point of the Mott MIT. In particular, the on-site moment as a proper order parameter can give a consistent description of two distinct forms of the critical points in the Mott MIT.

Models and Methods. The Hubbard model is the simplest model that captures the essential physics of MIT in a strongly correlated system. The Hamiltonian of the one-band Hubbard model is given by [17–20],

$$H = -t \sum_{\langle ij \rangle \sigma} d_{i\sigma}^\dagger d_{j\sigma} - \mu \sum_{i\sigma} d_{i\sigma}^\dagger d_{i\sigma} + \frac{U}{2} \sum_{i\sigma} n_{i\sigma} n_{i\bar{\sigma}}, \quad (1)$$

where the summation $\langle ij \rangle$ is over all sites i , and for each site i , restricted to its nearest-neighbor (NN) sites j , t denote the electron NN hopping amplitude, U is the on-site Coulomb repulsion between electrons, and μ is the chemical potential. $d_{i\sigma}^\dagger$ ($d_{i\sigma}$) is the creation (annihilation) operator for an electron with spin σ at lattice site i , and $n_{i\sigma}$ is the occupation number operator of electrons at lattice site i . Unless explicitly stated, we set $t = 1$ as the energy scale in this paper. The electron Green's function of the Hubbard model (1) can be expressed formally as,

$$G_\sigma(\mathbf{k}, \omega) = \frac{1}{\omega + \mu - \varepsilon_{\mathbf{k}} - \Sigma_\sigma(\mathbf{k}, \omega)}, \quad (2)$$

where the energy dispersion in the tight-binding approximation is obtained directly from the Hubbard model (1) as $\varepsilon_{\mathbf{k}} = -2t(\cos k_x + \cos k_y)$ for a square lattice, while the effect of interaction in the Hubbard model (1) has been encoded in the electron self-energy $\Sigma_{\sigma}(\mathbf{k}, \omega)$. It should be emphasized that in the infinite dimensional system, this electron self-energy $\Sigma_{\sigma}(\mathbf{k}, \omega)$ is momentum independent. However, DMFT [24, 25] provides an approximate solution to this electron self-energy $\Sigma_{\sigma}(\mathbf{k}, \omega)$ in a finite dimensional system by setting $\Sigma_{\sigma}(\mathbf{k}, \omega) = \Sigma_{\sigma}^{(\text{AIM})}(\omega)$, where the momentum independence of the electron self-energy (then the local electron self-energy) $\Sigma_{\sigma}^{(\text{AIM})}(\omega)$ can be obtained in terms of an auxiliary impurity model consisting of a single interacting site in a self-consistently determined bath [14]. In other words, the auxiliary impurity model provides a way to calculate the local electron self-energy $\Sigma_{\sigma}^{(\text{AIM})}(\omega)$ and to use the entire repertoire of the electron Green's function with the contribution to the electron self-energy taken from the auxiliary impurity system rather than from a perturbation expansion [26].

We evaluate the electron self-energy of the Hubbard model (1) in terms of DMFT with the *Lanczos* method as impurity solver. In the framework of DMFT, the Hubbard model (1) is mapped onto an effective single impurity model by dropping the nonlocal contribution to the electron self-energy,

$$H_{\text{imp}} = \sum_{m\sigma} \varepsilon_m c_{m\sigma}^{\dagger} c_{m\sigma} + \sum_{m\sigma} V_m (c_{m\sigma}^{\dagger} d_{\sigma} + d_{\sigma}^{\dagger} c_{m\sigma}) + \sum_{\sigma} (\varepsilon - \mu) d_{\sigma}^{\dagger} d_{\sigma} + \frac{U}{2} \sum_{\sigma} n_{\sigma} n_{\bar{\sigma}}, \quad (3)$$

which becomes exact in the limit of the infinite lattice coordination [21]. Here d_{σ}^{\dagger} (d_{σ}) creates (annihilates) a particle in the *impurity orbital* and $c_{m\sigma}^{\dagger}$ ($c_{m\sigma}$) creates (annihilates) an electron in a *conduction band*, where the *impurity orbital* and *conduction band* are coupled each other via effective parameters ε_m and V_m , which are determined by the self-consistent DMFT calculation utilizing an impurity solver. In the following discussions, we introduce the local electron Green's function in real-space as [22, 23],

$$\mathcal{G}_{\sigma}(\tau) = - < T_{\tau} d_{\sigma}(\tau) d_{\sigma}^{\dagger}(0) >, \quad (4)$$

with the imaginary time $\tau = it$. This local electron Green's function (4) in energy-space can be obtained directly in terms of the Fourier transformation as,

$$\mathcal{G}_{\sigma}(i\omega_n) = \int_0^{\beta} d\tau e^{i\omega_n \tau} \mathcal{G}_{\sigma}(\tau), \quad (5)$$

$$\mathcal{G}_{\sigma}(\tau) = \frac{1}{\beta} \sum_{n=-\infty}^{\infty} e^{-i\omega_n \tau} \mathcal{G}_{\sigma}(i\omega_n), \quad (6)$$

where $-\beta \leq \tau \leq \beta$ and the fermionic Matsubara frequency $\omega_n = (2n+1)\pi/\beta$ with $n = 0, \pm 1, \pm 2, \dots$.

The local properties of the Hubbard model on the Bethe lattice can be obtained via a single-site impurity problem supplemented by the following self-consistent relation [27, 28],

$$\mathcal{G}_{0\sigma}^{-1}(i\omega_n) = i\omega_n + \mu - t^2 \mathcal{G}_{\sigma}(i\omega_n), \quad (7)$$

where $\mathcal{G}_{0\sigma}$ is the bare Green's function. The self-consistent relation ensures that the on-site (local) component of the Green's function $[\mathcal{G}_{ii}(i\omega_n) = \frac{1}{N} \sum_k \mathcal{G}(\mathbf{k}, i\omega_n)]$ coincides with the Green's function $\mathcal{G}_{\sigma}(i\omega_n)$ calculated from the effective action.

The Green's function $\mathcal{G}_{\text{imp}}(i\omega_n)$ of the impurity model (3) is then calculated by the *Lanczos* method [29, 30], which can be expressed explicitly as [7, 27, 31],

$$\mathcal{G}_{\sigma, \text{imp}}(i\omega_n) = \mathcal{G}_{\sigma}^{+}(i\omega_n) + \mathcal{G}_{\sigma}^{-}(i\omega_n), \quad (8)$$

with $\mathcal{G}_{\sigma}^{+}(i\omega_n)$ and $\mathcal{G}_{\sigma}^{-}(i\omega_n)$ that are given by,

$$\mathcal{G}_{\sigma}^{+}(i\omega_n) = \frac{\langle \phi_0 | d_{\sigma} d_{\sigma}^{\dagger} | \phi_0 \rangle}{i\omega_n - a_0^{(+)} - \frac{b_1^{(+)^2}}{i\omega_n - a_1^{(+)} - \frac{b_2^{(+)^2}}{i\omega_n - a_2^{(+)} - \dots}}}, \quad (9)$$

$$\mathcal{G}_{\sigma}^{-}(i\omega_n) = \frac{\langle \phi_0 | d_{\sigma}^{\dagger} d_{\sigma} | \phi_0 \rangle}{i\omega_n + a_0^{(-)} - \frac{b_1^{(-)^2}}{i\omega_n + a_1^{(-)} - \frac{b_2^{(-)^2}}{i\omega_n + a_2^{(-)} - \dots}}}, \quad (10)$$

where a_n (b_n) is the n th sub-diagonal element of the tridiagonalized Hamiltonian obtained by the *Lanczos* method, and $|\phi_0\rangle$ is the ground state of the Hamiltonian (3). In our calculations, we choose $\beta = 1024$ to assure the accuracy of the self-consistency calculations, especially in the low-energy region.

The Green's function behaves differently depending on whether the eigenstates are localized or extended [32], which helps us to obtain the interaction effect on the phase transitions. For an interacting system, we introduce the *on-site moment* in terms of the Green's function $\mathcal{G}_{\sigma}(i\omega_n)$ as,

$$m_o = -\frac{1}{\beta} \sum_{n=-\infty}^{\infty} e^{i\omega_n 0^+} \sum_{\sigma} \sigma \mathcal{G}_{\sigma}(i\omega_n), \quad (11)$$

with $\sigma = \pm$ for spin-up or spin-down. The factor $e^{i\omega_n 0^+}$ is introduced to ensure the convergence of the summations.

In the metallic phase, the system is a Fermi liquid with the vanishing of the imaginary part of self-energy at the Fermi level [33]. Considering the electron occupation of the spin-up state is equal to that of the spin-down state for the *impurity orbital* when $\mathcal{G}_{\uparrow} = \mathcal{G}_{\downarrow}$, the on-site moment m_o keeps equal to zero in the metallic region. On the contrary, as we will discuss in more detail below, the ground state is double degenerated with different probabilities of the spin-up and spin-down singly occupied states, i.e. $\mathcal{G}_{\uparrow} \neq \mathcal{G}_{\downarrow}$ in the insulating phase, leading a

sudden rise of the on-site moment at the critical interaction U_c . Moreover, if the order parameter m_o does not change for a Mott insulator, it may be an *topological invariant* [35]. In that case, though the findings in Ref. [35] and our work are different, the two approaches lead to equally satisfactory results.

To evaluate the frequency summation over the Matsubara Green's function, we need to further simplify the above formula by considering the interacting Matsubara Green's function at the poles, which holds,

$$[\mathcal{G}_\sigma(i\omega_n)] = [\mathcal{G}_\sigma(-i\omega_n)]^*, \quad \omega_n = \frac{(2n+1)\pi}{\beta}, \quad n = 0, 1, 2, \dots \quad (12)$$

With the help of the above equation (12), the on-site moment at an any given site in Eq. (11) can be rewritten explicitly as,

$$m_o = -\frac{2}{\beta} \operatorname{Re} \sum_{n=0}^{\infty} e^{i\omega_n 0^+} \sum_{\sigma} \sigma \mathcal{G}_\sigma(i\omega_n), \quad (13)$$

which therefore shows that we can obtain the on-site moment m_o at an any given site directly from the summation of positive frequency in the effective on-site problem.

Mott MIT depicted by on-site moment. We define the quasiparticle coherent weight Z_F as [23, 36],

$$\frac{1}{Z_F} = 1 - \frac{\partial}{\partial \omega} \operatorname{Re} \Sigma_\sigma(\omega) |_{\omega=0} \approx 1 - \frac{\operatorname{Im} \Sigma_\sigma(i\omega_0)}{\omega_0}, \quad (14)$$

where the local self-energy $\Sigma_\sigma(i\omega_n)$ is obtained from the local Green's function in Eq. (7). In the following discussions, we study the Mott MIT of the Hubbard model at half-filling in terms of the evolution of the on-site moment m_o at an any given site with the on-site Coulomb repulsive interaction U . In Fig. 1 we plot m_o as a function of interaction U , where the red dashed-line indicates the position of the critical point of the Mott MIT. For a better comparison, the evolution of the quasiparticle coherent weight Z_F (blue solid-line) with U is also presented in Fig. 1. Z_F usually decreases with increasing U and keeps very close to zero when approaching the critical interaction U_c of the Mott MIT, near which the systematic errors of Z_F increases heavily, leading to a difficult problem for the quantitative determination of the critical point of MIT. More crucially, within the framework of DMFT, two metallic results with different slope dZ_F/dU are found to coexist in a finite range of interaction strengths [15, 16], and thus a comparing of the respective energies with the energy of the insulator is suggested [16]. Consequently, it becomes quite difficult and inconvenient to numerically determine the actual critical interaction U_c by the quasiparticle coherent weight. In a striking contrast to the complex of Z_F that has two metallic solutions in the coexistence region of interaction U , the on-site moment m_o keeps equal to zero for both the metastable and stable metallic solutions when $U < U_c$,

as shown in Fig. 1. However, at the critical point $U_c=6.5$ of MIT, the on-site moment jumps abruptly from $m_o = 0$ in the metallic phase to $m_o \approx 1$ in the insulating phase. Our results indicate clearly that the on-site moment m_o at an any given site is very sensitive to the existence of the resonant-peak at Fermi level, which therefore is a more proper order parameter to quantitative depict the critical point of the Mott MIT.

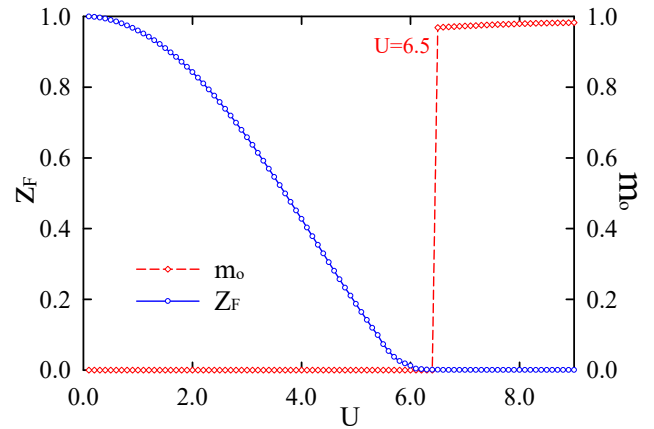


FIG. 1. (Color online) The on-site moment m_o (red dotted-line) as a function of interaction U . MIT happens when $U_c=6.5$ and $\beta = 1024$. For a comparison, the evolution of the quasiparticle coherent weight Z_F with U (blue solid-line) is also presented.

Two classes of solutions. Now we turn to discuss the two classes of solutions: (i) the solution from the metallic phase towards the critical interaction of MIT (the metallic-phase solution U_{c2}); and (ii) the solution from the insulating phase towards the critical point of MIT (the insulating-phase solution U_{c1}), and then show that the on-site moment m_o as a more proper order parameter of MIT can give a natural explanation of the difference between the metallic and insulating solutions. In this case, we have made a series of calculations for m_o , and the results of the metallic solution of m_o (red dotted-line) and the insulating solution (blue solid-line) are plotted in Fig. 2, where $U_{c1} = 4.7$ and $U_{c2} = 6.5$ are the critical points of the insulator to metal transition and metal to insulator transition, respectively. Our findings of the critical interactions U_{c1} and U_{c2} are in agreement with the DMFT results near the zero temperature [37]. These results in Fig. 2 show that apart from a metallic phase at the weak interaction region ($U < U_{c1}$) and a insulating phase at the strong interaction region ($U > U_{c2}$), there is an intermediate interaction region ($U_{c1} < U < U_{c2}$), where the metallic solution coexists with the insulating solution. Within this intermediate interaction region, m_o as a function of U exhibits a hysteretic behavior since both the metallic and insulating solutions are found to be attractive points of a particle-hole symmetry system

[14]. The present results in Fig. 1 and Fig. 2 therefore show that m_o is a more proper order parameter to give a quantitative description of the Mott MIT in a strong correlation system.

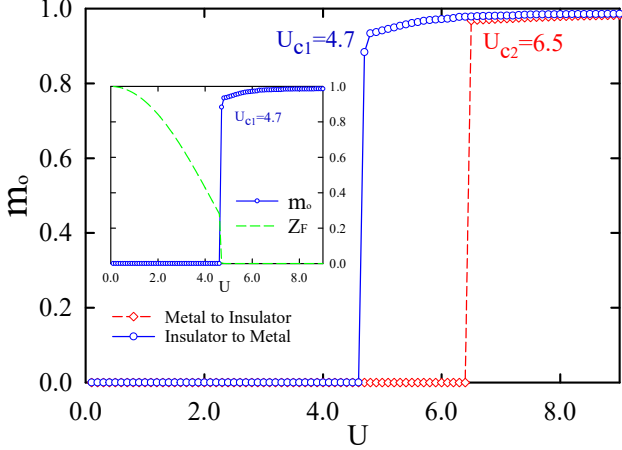


FIG. 2. (Color online) The on-site moment m_o as a function of interaction U . The blue line indicates the critical point at $U_{c1} = 4.7$, while the red line denotes the critical point at $U_{c2} = 6.5$. Within the region between the two critical points of U_{c1} and U_{c2} , the insulating solution (blue solid-line) and metallic solution (red dotted-line) coexist. Inset: The comparison of the on-site moment (blue solid-line) and the quasiparticle coherent weight (green dotted-line) for the insulating-phase solution.

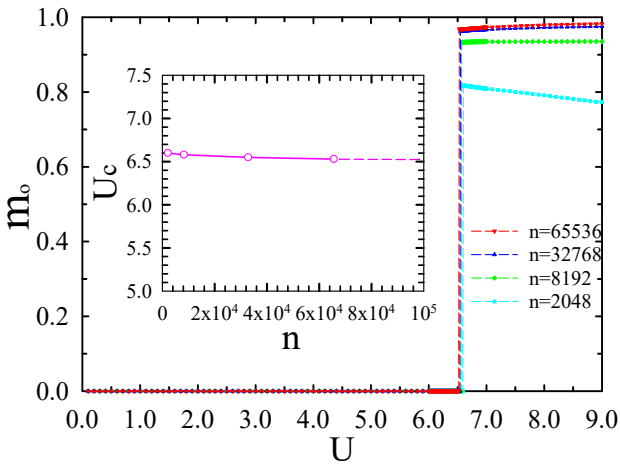


FIG. 3. (Color online) A comparison of the on-site moment m_o as a function of interaction U with different cutoff n of the series summation. The evolution of U_c with n (circles) is shown (inset) along with the fitting line (solid line) and its extension (dashed line).

Now we estimate the cutoff effect. This follows a basic fact that although the summation of Matsubara frequency in equation (13) is from zero to infinity, the ac-

tual calculation is performed numerically with the infinitude of Matsubara frequency $n = 0, 1, 2, \dots, \infty \rightarrow n = 0, 1, 2, \dots, n_{max}$ replaced by a finite n_{max} . In this case, we have made a series of calculations for m_o as a function of U at different cutoff n_{max} , and the results are plotted in Fig. 3, where the critical points at $n_{max} = 2048$, $n_{max} = 8192$, $n_{max} = 32768$, and $n_{max} = 65536$ are very close to each other, indicating that for the large enough n_{max} , the error bars are small enough. In particular, U_c can be extrapolated as $U_c = 6.5$ in the case of $n_{max} = \infty$.

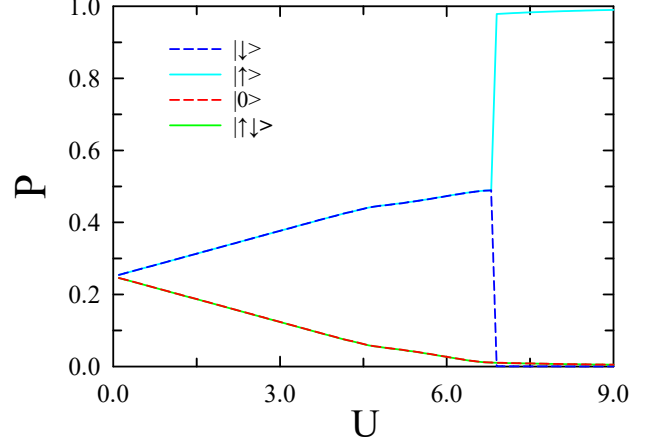


FIG. 4. (Color online) The probabilities P of the zero occupied state $|0\rangle$ (red dashed line), spin-up occupied state $|\uparrow\rangle$ (cyan solid line), spin-down occupied state $|\downarrow\rangle$ (blue dashed line), and double occupied state $|\uparrow\downarrow\rangle$ (green solid line) at the single impurity site as a function of interaction U .

The Hilbert space of each site in the Hubbard model (1) consists of four states, $|0\rangle$, $|\uparrow\rangle$, $|\downarrow\rangle$, $|\uparrow\downarrow\rangle$, corresponding to the zero, spin-up, spin-down, and double electron occupied states, respectively. For a further understanding of the nature of MIT occurred in the Hubbard model, the probabilities of the zero, spin-up, spin-down, and double occupied states at the single impurity site of the metallic solution are plotted in Fig. 4, where shows clearly that the probabilities of the zero and double occupied states are equal in the metallic phase, however, the probability of the spin-up singly occupied state increases with the increase of the on-site Coulomb interaction U and jumps to $P \approx 1$ at the critical point $U_{c2} = 6.5$. The same feature for the probability of the spin-down singly occupied state is found in the insulating phase due to the degeneration. Concomitantly, the on-site moment is equal to zero when the probability of the spin-up singly occupied state is equal to that of the spin-down singly occupied state (then $\mathcal{G}_\uparrow = \mathcal{G}_\downarrow$) in the metallic phase. However, in a striking contrast to the case in the metallic phase, the feature of the probability of the spin-up singly occupied state is quite different from that of the probability of the spin-down singly oc-

cupied state in the insulating phase, and a jump of the on-site moment is found at the critical point due to the presence of two possible solutions with $\mathcal{G}_\uparrow \neq \mathcal{G}_\downarrow$. This is why the on-site moment in Eq (11) is a more proper order parameter to give a quantitative depiction of two distinct forms of the critical points in MIT of a strongly correlated system.

Conclusions. Based on the one-band Hubbard model, we have studied the Mott MIT in a strong correlation system in terms of the combined DMFT and Lanczos technique. Our results show very clearly that the on-site moment as a proper order parameter can correctly depict the Mott MIT in a strong correlation system, including the quantitative determination of the critical points as well as the consistent description of two distinct forms of the critical points. The on-site moment is a universal order parameter of strong correlation systems, and can be also used to discuss the novel physics in orbital-selective Mott insulators [38] and superconductors [39, 40]. In particular, it may be applied to explain the hysteresis observed experimentally from the Mott-field effect transistors [41, 42], and these related works are under investigation now.

ACKNOWLEDGEMENTS

The authors would like to thank Gabriele Bellomia for fruitful discussions. YN is also grateful to Louk Rademaker, Haiming Dong, Quanjie Zhong, and Huan Xu for helpful discussions. This work is supported by the Fundamental Research Funds for the Central Universities of China under Grant No. JN200208. YS is supported by the National Natural Science Foundation of China (NSFC) under Grant No. 11474023. SF is supported by the National Key Research and Development Program of China under Grant No. 2021YFA1401803, and NSFC under Grant Nos. 11974051 and 11734002.

Rev. Lett. **83**, 136 (1999); R. Bulla, and M. Potthoff, "Linearized" dynamical mean-field theory for the Mott-Hubbard transition, Eur. Phys. J. B **13**, 257 (2000).

[6] V. Turkowski, *Dynamical Mean-Field Theory for Strongly Correlated Materials* (Springer Nature Switzerland AG, 2021).

[7] See, e.g., the review, A. Georges, G. Kotliar, W. Krauth, and M. J. Rozenberg, Dynamical mean-field theory of strongly correlated fermion systems and the limit of infinite dimensions, Rev. Mod. Phys. **68**, 13 (1996).

[8] S. Florens, A. Georges, G. Kotliar, and O. Parcollet, Mott transition at large orbital degeneracy: Dynamical mean-field theory, Phys. Rev. B **66**, 205102 (2002).

[9] M. Feldbacher, K. Held, and F. F. Assaad, Projective Quantum Monte Carlo Method for the Anderson Impurity Model and its Application to Dynamical Mean Field Theory, Phys. Rev. Lett. **93**, 136405 (2004).

[10] C. Raas and G. S. Uhrig, Generic susceptibilities of the half-filled Hubbard model in infinite dimensions, Phys. Rev. B **79**, 115136 (2009).

[11] G. Sordi, K. Haule, and A.-M. S. Tremblay, Mott physics and first-order transition between two metals in the normal-state phase diagram of the two-dimensional Hubbard model, Phys. Rev. B **84**, 075161 (2011).

[12] H. Eisenlohr, S.-S. B. Lee, and M. Vojta, Mott quantum criticality in the one-band Hubbard model: Dynamical mean-field theory, power-law spectra, and scaling, Phys. Rev. B **100**, 155152 (2019).

[13] S. Zhou, L. Liang, and Z. Wang, Dynamical slave-boson mean-field study of the Mott transition in the Hubbard model in the large- z limit, Phys. Rev. B **101**, 035106 (2020).

[14] E. G. C. P. van Loon, F. Krien, and A. A. Katani, Bethe-Salpeter equation at the critical end point of the Mott transition, Phys. Rev. Lett. **125**, 136402 (2020).

[15] M. Chatzileftheriou, A. Kowalski, M. Berović, A. Amaricci, M. Capone, L. De Leo, G. Sangiovanni, and L. de' Medici, Mott Quantum Critical Points at finite doping, arXiv: 2203.02451.

[16] Y. Ono, M. Potthoff, and R. Bulla, Mott transitions in correlated electron systems with orbital degrees of freedom, Phys. Rev. B **67**, 035119 (2003).

[17] J. Kanamori, Electron Correlation and Ferromagnetism of Transition Metals, Progress of Theoretical Physics **30**, 275 (1963).

[18] J. Hubbard, Electron correlations in narrow energy bands, P. Roy. Soc. Lond. A **276**, 238 (1963).

[19] J. Hubbard, Electron correlations in narrow energy bands. II. The degenerate band case, P. Roy. Soc. Lond. A **277**, 237 (1964).

[20] J. Hubbard, Electron correlations in narrow energy bands. III. An improved solution, P. Roy. Soc. Lond. A **281**, 401 (1964).

[21] A. Georges and G. Kotliar, Hubbard model in infinite dimensions, Phys. Rev. B **45**, 6479 (1992).

[22] V. Anisimov and Y. Izyumov, *Electronic Structure of Strongly Correlated Materials* (Springer-Verlag Berlin Heidelberg, 2010).

[23] G. D. Mahan, *Many-Particle Physics* (World Book Inc, 2000).

[24] E. Muller-Hartmann, Correlated fermions on a lattice in high dimensions, Z. Phys. B **74**, 507 (1989).

[25] W. Metzner and D. Vollhardt, Correlated lattice fermions in $d = \infty$ dimensions, Phys. Rev. Lett. **62**, 324 (1989).

* nyk@cumt.edu.cn

† yunsong@bnu.edu.cn

‡ spfeng@bnu.edu.cn

[1] N. F. Mott, The Basis of the Electron Theory of Metals, with Special Reference to the Transition Metals, Proceedings of the Physical Society. Section A **62**, 416 (1949).

[2] See, e.g., the review, N. F. Mott, Metal-Insulator Transition, Rev. Mod. Phys. **40**, 677 (1968).

[3] See, e.g., the review, M. Imada, A. Fujimori, and Y. Tokura, Metal-insulator transitions, Rev. Mod. Phys. **70**, 1039 (1998).

[4] W. F. Brinkman and T. M. Rice, Application of Gutzwiller's Variational Method to the Metal-Insulator Transition, Phys. Rev. B **2**, 4302 (1970).

[5] R. Bulla, Zero Temperature Metal-Insulator Transition in the Infinite-Dimensional Hubbard Model, Phys.

[26] Richard M. Martin and Lucia Reining and David M. Ceperley, *Interacting Electrons* (Cambridge University Press, 2016).

[27] M. Caffarel and W. Krauth, Exact diagonalization approach to correlated fermions in infinite dimensions: Mott transition and superconductivity, *Phys. Rev. Lett.* **72**, 1545 (1994).

[28] L. Laloux, A. Georges, and W. Krauth, Effect of a magnetic field on Mott-Hubbard systems, *Phys. Rev. B* **50**, 3092 (1994).

[29] E. Dagotto, Correlated electrons in high-temperature superconductors, *Rev. Mod. Phys.* **66**, 763 (1994).

[30] Y. Niu, J. Sun, Y. Ni, J. Liu, Y. Song, and S. Feng, Doublon-holon excitations split by Hund's rule coupling within the orbital-selective Mott phase, *Phys. Rev. B* **100**, 075158 (2019).

[31] M. Capone, L. de' Medici, and A. Georges, Solving the dynamical mean-field theory at very low temperatures using the Lanczos exact diagonalization, *Phys. Rev. B* **76**, 245116 (2007).

[32] E. N. Economou, *Green's Functions in Quantum Physics* (Springer-Verlag Berlin Heidelberg, 2006).

[33] D. E. Logan, and M. R. Galpin, Mott insulators and the doping-induced Mott transition within DMFT: exact results for the one-band Hubbard model, *Journal of Physics: Condensed Matter* **28**, 025601 (2016).

[34] M. Yuta, E. Martin, and W. Philipp, High-Harmonic Generation in Mott Insulators, *Phys. Rev. Lett.* **121**, 057405 (2018).

[35] S. Sen, P. J. Wong, and A. K. Mitchell, The Mott transition as a topological phase transition, *Phys. Rev. B* **102**, 081110(R) (2020).

[36] C. A. Perroni, H. Ishida, and A. Liebsch, Exact diagonalization dynamical mean-field theory for multiband materials: Effect of Coulomb correlations on the Fermi surface of $Na_{0.3}CoO_2$, *Phys. Rev. B* **75**, 045125 (2007).

[37] H. U. R. Strand, A. Sabashvili, M. Granath, B. Hellsing, and S. Bo and Östlund, Dynamical mean field theory phase-space extension and critical properties of the finite temperature Mott transition, *Phys. Rev. B* **83**, 205136 (2011).

[38] See, e.g., the review, G. Kotliar, S. Y. Savrasov, K. Haule, V. S. Oudovenko, O. Parcollet, and C. A. Marianetti, Electronic structure calculations with dynamical mean-field theory, *Rev. Mod. Phys.* **78**, 865 (2006).

[39] See, e.g., the review, P. A. Lee, N. Nagaosa, and X.-G. Wen, Doping a Mott insulator: Physics of high-temperature superconductivity, *Rev. Mod. Phys.* **78**, 17 (2006).

[40] See, e.g., the review, A. H. Castro Neto, F. Guinea, N. M. R. Peres, K. S. Novoselov, and A. K. Geim, The electronic properties of graphene, *Rev. Mod. Phys.* **81**, 109 (2009).

[41] H.-T. Kim, B.-G. Chae, D.-H. Youn, S.-L. Maeng, G. Kim, K.-Y. Kang, and Y.-S. Lim, Mechanism and observation of Mott transition in VO_2 -based two- and three-terminal devices, *New Journal of Physics* **6**, 52 (2004).

[42] S. B. Roy, *Mott Insulators Physics and applications* (IOP Publishing, 2019).